



An electrochemical study of acrylate bone adhesive permeability and selectivity change during *in vitro* ageing: A model approach to the study of biomaterials and membrane barriers

M. Raja ^{a,*}, J.C. Shelton ^a, F. Salamat-Zadeh ^b, M. Tavakoli ^c, S. Donell ^d, G. Watts ^e, P. Vadgama ^a

^a School of Materials and Engineering Science, Queen Mary University of London, Mile End Road, London, E1 4NS, UK

^b TWI, Granta Park, Great Abington, Cambridge, CB21 6AL, UK

^c KTN LTD, Suite 220 Business Design Centre, 52 Upper Street, London, N1 0QH, UK

^d University of East Anglia, Norwich Research Park, Norwich, Norfolk, NR4 7TJ, UK

^e Liverpool John Moores University, Byrom Street, Liverpool, L3 3AF, UK

ARTICLE INFO

Article history:

Received 17 December 2018

Received in revised form

20 February 2019

Accepted 26 February 2019

Available online 4 March 2019

Keywords:

Bone fracture fixation

Acrylate adhesive ageing

Adhesive joint strength testing

Cyclic voltammetry

Chronoamperometry

Diffusion coefficient

ABSTRACT

This study assessed the solute permeability of a family of UV and moisture cured acrylates-based adhesives during *in vitro* ageing in pH 7.4 buffer. Acrylates have a potential role in bone fracture fixation, but their inability to allow microsolite exchange between the fractured bone surfaces may contribute to ineffective healing. Cyclic voltammetry and chronoamperometry were used to determine the diffusion coefficients for various electrochemically active probe molecules (O₂, H₂O₂, acetaminophen, catechol, uric acid and ascorbic acid) at proprietary acrylic, urethane – acrylate and cyanoacrylate adhesives. All adhesives proved to be impermeable for up to 9 days ageing, following which a near-exponential increase in permeability resulted for all solutes. At 18 days, the diffusion coefficients were in the range of 10⁻⁵ cm²s⁻¹ for O₂ and H₂O₂ and 10⁻⁶ cm²s⁻¹ for the organic solutes; no transport selectivity was seen between the latter. Adhesive joint strength showed a direct, inverse, correlation with permeability, with the more hydrophilic cyanoacrylates showing the greatest loss of strength. Adhesive permeabilisation does not appear to be compatible with the retention of bonding strength, but it serves as a new non-destructive predictor of adhesion strength change during ageing and practical use.

© 2019 The Authors. Published by Elsevier B.V. This is an open access article under the CC BY-NC-ND license (<http://creativecommons.org/licenses/by-nc-nd/4.0/>).

1. Introduction

The integrity of polymeric materials, whether used as implants with mechanical properties [1] or barrier layers to control sample-biosensor diffusional exchange [2], are strongly influenced by hydration and later degradation. Regardless of application, a feature of any polymer, no matter how dense its polymeric network, is the change in its small molecule permeability during water uptake. We selected an important polymer class, bone adhesives, which as applied thin layers have attributes that can be referenced against both solute permeability and mechanical strength.

Bone fractures are a major cause of disability and present substantial pressures on health care services. In the US alone, there are

an estimated 1.5 million fracture cases per annum leading to health costs of \$17bn, and now with more active lifestyles, these figures are projected to increase by 50% in 2040 [3]. Standard fixation of fractures using metal plates and screws ensure stable positioning for bone healing and are particularly suited to fractures of major long bones, but adhesives are being actively investigated as an alternative as injectable, conformal, bonding agents, requiring no further invasive procedure.

There is ongoing development of polymer-based adhesives for bone fixation, and specifically, adhesives that can undergo rapid *in vivo* setting, minimizing open surgical intervention and associated extended inpatient stays. However, these adhesives have not to-date provided the joint strength needed for weight bearing bones [4], but offer a high potential value in fixation of non-weight bearing small bones, particularly where the anatomy is complex. Following injection, ideally, an adhesive is fully resorbed to allow complete biological bridging by the newly formed repair hard

* Corresponding author.

E-mail address: m.a.a.raja@qmul.ac.uk (M. Raja).

List of abbreviations

CA	Cyanoacrylate
AU	Acrylate-Urethane
CV	Cyclic Voltammetry
PBS	Phosphate-Buffered Saline
MW	Molecular weight
DM	Dialysis Membrane
AM	Adhesive Membrane
DC	Diffusion Coefficient

tissue (callus). However, there is a balance to be reached between a water resisting adhesive, and one that allows water and solute ingress to enable biological crosstalk between fracture surfaces. Tissue remodelling, generally, requires active molecular signalling and solute cues mediated by cytokine and small molecule gradients and concentrations [5,6]. Remarkably, we know little about either permeability or permeability change at such materials. Additionally, adhesives will degrade in water, and the rate of this has implications for adhesion lifetime *in vivo* and progress towards increased permeabilisation for better fracture healing. In the case of rapidly curing acrylate adhesives, it is well known that hydration leads to degradation, in either water or moisture [7,8], but the permeability correlation with strength is unknown. There are parallels here with the hydration and degradation of polymeric membranes used for implantable glucose biosensors which are exquisitely dependent on barrier membrane permeability [9].

This *in vitro* study focussed on the dry to wet stage permeability change at a precision designed bovine bone model using acrylate adhesives, an adhesive group that is already of considerable medical interest for soft tissue bonding, but with potential for small bone repair and with potential as a formable sensing barrier membrane, though that was not the focus of this present study. A study question was, can electrochemical monitoring be applied to tracking diffusion through a highly diffusional resistant polymer. In accordance with this, an important adhesive sub-group was targeted: cyanoacrylates. These have been extensively studied previously [10], and their adhesive potential recognised in the 1950s, with a commercial product (Eastman 910[®]) emerging in 1958. Their suitability is partly based on low viscosity so penetration of voids and cavities in adherends is facilitated [11] and partly on structural versatility, achieved through functional side group variation. They are appropriate for bone because of its high surface voids, and because side chain modification should allow tailoring of strength, water uptake and degradation. It is known that longer side chains provide higher strength and slower degradation [12–15], with butyl-cyanoacrylates, for example, giving longer term strength than ethyl-cyanoacrylates [16–18] and a reduced degradation rate than methyl-cyanoacrylates [19], but permeability correlates are unknown.

Whilst acrylates retain adhesive properties under wet conditions [10], the toxicity of their degradation products is a concern. Hydrolysis, even in physiological buffer generates formaldehyde and cyanoacetate [20,21], although in *in vivo* deployment esterases lead to the generation of lower toxicity alcohol and poly(cyanoacrylic) acid [15,22,23]. There are also operational variations; isobutyl 2-cyanoacrylate avoids toxic tissue effects [24], whilst butyl-2-cyanoacrylate provokes evident tissue inflammation [25] and short chain cyanoacrylate is directly cytotoxic [26,27].

At one extreme, complete fracture surface sealing by an adhesive will retard bone repair [28], emphasising the need for tissue solute exchange. Two adhesives types were considered in the

present study. First, those with acrylate groups ($\text{CH}_2=\text{CHCOO}^-$) as in acrylic. Second, urethane-acrylate adhesives which undergo free radical polymerisation under UV in the presence of photoinitiator and cyanoacrylates (CAs) with electron withdrawing $-\text{COOCH}_3$ and $-\text{CN}$ groups to allow anionic polymerisation in moisture [29,30]. Also, as adhesives are known to hydrate and take up water, an underlying aim was to understand the effect of water ingress [31]. The 'dry to wet' conversion is known to lead to strength loss and ultimately adhesive failure; the penetration of water alone can lead to swelling and stresses within the interlocking surfaces [32,33], so reducing the efficacy of the adhesive prior to degradative porosity increase. If these materials are to be introduced as biosensor materials more widely [34] further insight into ageing effects are warranted. We combined cyclic voltammetric [35] and chronoamperometric [36,37] measurements of simple probe molecules for non-destructive tracking of permeability changes (bulk property) and later correlated this with destructive mechanical testing of adhesion (surface property) at bone surfaces.

We proposed to study the nature of the partial sealing associated with degrading acrylate adhesives during ageing, never previously considered. With cyclic voltammetry, peak current was used to obtain diffusion coefficients through the Randles-Sevcik equation:

$$i_p = (2.686 \times 10^5) n^{3/2} \nu^{1/2} D^{1/2} A C \quad (1)$$

Where i_p is peak current, n is the number of electrons, ν is the scan rate, D is diffusion coefficient, A is electrode surface area and C is solute bulk concentration [38–43]. The second approach utilising chronoamperometry used transient, dynamic electrode responses to step changes in target molecule concentration. With this latter approach we monitored and matched responses on a real time basis against model simulated responses incorporating Fick's Laws. We have previously reported on software to achieve this based on a bipartite, time partitioned, solution to Fick's Laws that combines speed, repeatability and simplicity [37,44–49].

Permeability determination at barrier membranes require high electrolyte permeability across the membrane to create a three electrode cell with the working electrode on the detection side and the counter and reference electrode on the bulk solution side. The barrier adhesive films used in the project had an extremely low micro-solute diffusion coefficients, so a different arrangement for the electrode cell was needed. This utilised an internal dialysis membrane as the electrolyte carrier allowing all three electrodes to be placed internal to the barrier layer. Whilst permeability analysis has been reported for low permeability materials, this has not previously used amperometry and has reported, for example, potentiometric interfacial measurement for ion permeability [50] and conductivity for water vapour permeability [51]. Certainly, O_2 permeability has been measured at various membrane barriers by amperometry, but this is at high permeability materials, e.g. Nafion [52]. The electrochemical rig used here enabled precision measurement of crystalloid and O_2 diffusion coefficients at ultra-low values. The work, moreover provides the first bridging communication linking material permeability/porosity with a material mechanical property. It has also shown that in contrast to the latter, a logarithmic scale increase in permeability provides a much higher sensitivity to materials ageing, at least in the case of adhesives, than mechanical testing. Whilst polymers tend to have high permeability to low polarity gas molecules compared with permeability to other microsolute, this is the first study to also show that despite its relatively high polarity H_2O_2 (dipole 2.2 D), its permeability approximates to the O_2 rather than to the other tested small solutes including catechol (dipole 2.6 D). In the context of biomaterials, the closest system with a low permeability to be studied

are dental adhesives and resins, but here the permeability properties focus on H₂O ingress and transport, and not solute transport [53]. Also, whilst there have been quantitative diffusion coefficient measurements through polymer membranes such as cellulose acetate, these have focused on providing a biological model [54] or for use in gas separation.

2. Experimental details

2.1. Materials and reagents

Di-sodium hydrogen phosphate (Na₂HPO₄), sodium dihydrogen phosphate (NaH₂PO₄), sodium chloride (NaCl) and sodium hydroxide solution (NaOH), were supplied by BDH (Dorset, UK). Deionised water was used for solution preparation and contact angle measurements. All experimental reagents; acetaminophen (analytical standard), L-ascorbic acid (reagent grade, crystalline), pyrocatechol ($\geq 99\%$), hydrogen peroxide solution (30 wt % in H₂O, ACS reagent), and uric acid ($\geq 99\%$, crystalline) were obtained from Sigma-Aldrich (Dorset, England).

All measurements were undertaken in phosphate buffer (PBS, 0.1 M, pH 7.4). Various stock solutions of 500 mM and 10 mM of the analytes, acetaminophen, L-ascorbic acid, pyrocatechol, hydrogen peroxide solution, and uric acid, were prepared in 0.1 M PBS and stored at 5 °C.

For oxygen sensing, 50 ml of 0.1 M PBS was purged with nitrogen (N₂) gas to fully deoxygenate the solution and internal electrolyte film of the adhesive membrane covered electrodes. The deoxygenated solution was sealed with Parafilm[®] and stored at 5 °C prior to use. For the diffusion studies, a separate 50 ml of 0.1 M PBS solution was air equilibrated and injected into the deoxygenated solution, which had been purged with nitrogen bubbling.

Cellulose dialysis tube membrane of flat width 76 mm was obtained from Sigma-Aldrich (Dorset, England). Glass microscope slides (75 × 50 mm, Corning[®], USA) were used to cast adhesive films. To create fixed depth adhesive layers, 50 μm diameter wire was used as spacer. Platinum wires with porous Teflon tips (CH Instruments Inc., USA) were utilised as counter electrodes. Parafilm[®] (Bemis, USA) and Sellotape Original Tape (Henkel) were used to seal open vessels.

Proprietary medical grade acrylate adhesives (both moisture and UV curable) were provided by Henkel Ltd (Hemel Hempstead, UK) (Table 1).

2.2. Strength characterisation

Bone diaphyses from bovine metacarpus was rough-cut and then ground utilising a sequence of P60 – P800 (Klingspor Abrasives Inc., USA) papers and finally polished with a sequence of P1000 – P4000 silicon carbide papers (Struers Ltd, UK) to obtain 5 × 5 × 20 mm cuboids. For adhesive joint strength testing, the adhesive was applied to bone overlap areas of 5 mm × 7 mm for lap shear testing and to a 5 mm × 5 mm area for butt joint testing.

Acrylate adhesive bonds optimally at thicknesses of <1 mm, so fixed, low, adhesive depth was ensured by using spacer wires of 50 μm diameter. Moisture-cured adhesive was left for 24 h at room temperature before testing. For UV curing, sequential 5 min UV exposure of each joint edge was carried out using an Omnicure Series 1500 light -curing lamp (EXFO Inc., Canada) and left for 24 h before testing.

Adhesive joint strengths were determined using a mechanical testing machine (Instron 5967 Dual Column Tabletop Universal Testing System, Instron, United Kingdom), with a cross-head speed of 0.5 mm/min.

2.3. Electrochemical measurements

An inverted oxygen Electrode (Rank Brothers Ltd., UK) was used for electrochemical analysis. A potentiostat (PalmSen, The Netherlands) was used for the voltammetry experiments. The potentiostat was software controlled using PSTrace software (PalmSen, The Netherlands).

To create adhesive based membranes for electrochemical measurements, preparations of defined thickness were made by applying adhesive solution to a 75–80 mm strip of dialysis membrane, with a second dialysis membrane placed on top using two spacers (10 mm from each end). The laminate was allowed to cure (Section 2.2) whilst sandwiched between two microscope slides. A Stereo Microscope (Leica Microsystems, Germany) was used for cross sectional examination of the cured adhesive laminate (Fig. 2). A laser micrometre (Mitutoyo, Hampshire, UK) was used for thickness measurements of the generated adhesive membranes.

Diffusion coefficient measurements of target molecules were carried out with only a dialysis membrane covered working to establish inherent dialysis membrane permeability prior to use of the laminate tri-layer of dialysis membrane-adhesive-dialysis membrane. Membranes were pre-soaked in 0.1 M PBS solution for 10 min to ensure electrolyte loading into the dialysis membrane to serve as a bridging electrolyte between the Pt working and Ag/AgCl reference electrode. The latter had the format of a partial ring round a Pt disc and was set back from the plane of the working electrode (Fig. 1). A platinum wire immersed in the solution above the Pt served as the counter electrode for the CV studies. Assays used 5 ml PBS solution, and each CV based diffusion determination used 10 independent voltage sweeps.

For chronoamperometry, the cell set up was similar, except that the Ag/AgCl ring now served as a combined counter/reference electrode. A polarising voltage of +0.65 V vs. Ag/AgCl was used for ascorbate, H₂O₂, acetaminophen, uric acid and catechol and of –0.65 V vs. Ag/AgCl for oxygen. Three rapid syringe injections, 50 μl of 0.5 M analyte stock solution, were made in stirred solution to give concentration jumps in 5 mM steps. Air equilibrated buffer volumes were injected into de-oxygenated buffer for the O₂ increments.

For the CV measurements, laminate covered electrodes were first incubated for 70 min in assay solution to allow target molecule

Table 1
Adhesives used along with their known monomers.

Chemical Type	Cure Method/Trade Name	Reported Monomers
Acrylate-Urethane	UV Cure: Loctite 3301	Isobornyl Acrylate 2-Hydroxyethyl acrylate Urethane-acrylate oligomer (Proprietary)
Acrylic	UV Cure: Loctite 3926	Isobornyl Acrylate 2-Hydroxyethyl acrylate
Cyanoacrylate	Moisture Cure: Loctite 4011, UV Cure: Loctite 4304	Ethyl 2-Cyanoacrylate

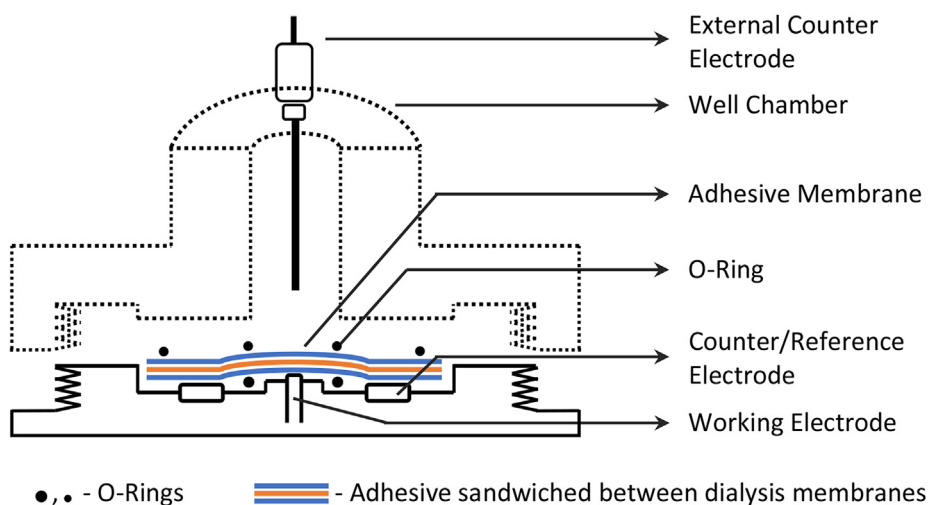


Fig. 1. Schematic of cross-sectional view of the cell setup for modified electrode.

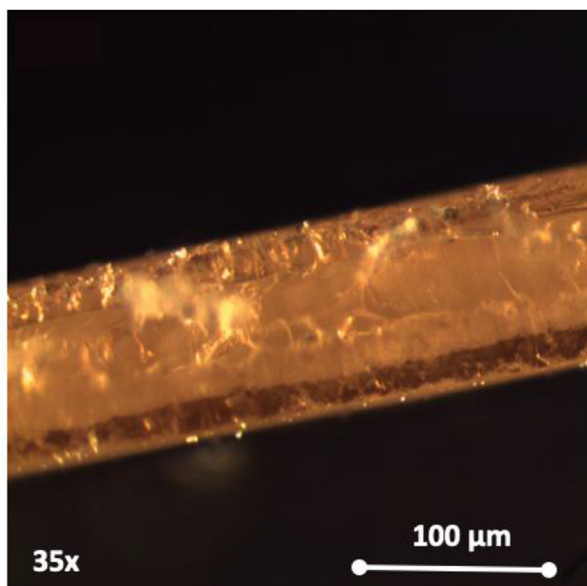


Fig. 2. Stereomicroscopic cross section of adhesive layer laminate with dialysis membranes shown at higher magnification without glass slides.

equilibration within the laminate. This time interval was based on the maximum observed period needed for completion to plateau of amperometric responses at the same membranes during the amperometric studies. In order to maintain consistency and to avoid any complications, film deposition on electrodes due to (non-reversible) solute oxidation, only the first cycle was used for each diffusion coefficient calculation.

2.4. Contact angle analysis

Adhesive polymer was applied to glass microscope slides with a rocking motion to achieve uniform spread prior to curing. Contact angle measurements were carried out at room temperature using a deionised water drop applied via instrumented controlled needle flow on a Drop Shape Analyzer (DSA100, KRÜSS GmbH, Germany) with a goniometer/image capture facility. Sessile drop fitting analysis was undertaken using the instrument program to establish contact angle of water drop. Ten readings were taken of each drop

during first 5 s of drop application. Seven repeat measurements were taken for each contact angle value determination.

2.5. Ageing

Adhesively-bonded joints and adhesive membranes were immersed in 100 mM phosphate buffered saline (pH 7.4) and stored in the ovens at 37 °C for 18 days (Precision™ Compact Ovens). The joints and membranes were removed from the ovens every 3 days and tested for strength and permeability.

3. Results

3.1. Imaging

Fig. 2 shows stereomicroscopic images of a cross section of adhesive layer laminates. The thickness of the adhesive membrane laminates was $100 \pm 0.004 \mu\text{m}$. Dialysis membrane pieces were used as permeable supporting structures for the adhesives. The molecular weight cut off (MWCO: 12,400) of these membranes was well above that of the probe molecules, and their permeability was established being greater than an order of magnitude of the values for the adhesive layers, allowing their added barrier effects to be disregarded.

3.2. Contact angle measurement

Sup. 1 shows the contact angles recorded for drop formation of water on each adhesive. For cyanoacrylate (CA) adhesives, Loctite 4011 and Loctite 4304, there were no significant differences between contact angles. Loctite 3926, an acrylate only adhesive, showed the highest contact angle and was significantly different from both the acrylate-urethane (AU) adhesive and the cyanoacrylate adhesives.

3.3. Electrochemical measurements

3.3.1. Chronoamperometry

The current-time profile provides an overall visual check on analyte diffusion and its consistency with a single rate-limiting Fickian diffusion barrier (Sup. 2). Dialysis membrane covered electrodes displayed a steep response rise, signifying fast analyte diffusion and stable steady state response were achieved under the

stirring conditions and sample volume used. Laminate covered working electrodes on the other hand displayed slowly rising currents (Sup. 2b), but again gave steady state responses. Observed response times varied, depending on probe molecular weight, with the smaller oxygen and hydrogen peroxide, generating steeper response profiles than the organics (acetaminophen, ascorbic acid, catechol, uric acid). Whilst with a dialysis membrane covered electrode, a current response was initiated immediately on analyte addition, the laminate covered electrodes showed an extended lag phase before registering a response, e.g. a response for organics initiated at 70 min on day 9 and at 20 min on day 18. For oxygen and hydrogen peroxide, responses were triggered at 40 min on day 6 and 10 min on day 18. There was a consistency across the organics suggesting that size alone, and not charge or polarity determined solute ingress.

3.3.2. Cyclic voltammetry

Preliminary diffusion studies with bare and dialysis membrane covered electrodes were conducted to establish baseline voltammograms.

The cyclic Voltammogram of acetaminophen (Fig. 3) displayed reversible behaviour with defined anodic (oxidation) ($E_{pa} = 0.85$ V) and cathodic (reduction) ($E_{pc} = 0.17$ V) peaks. The observed peak separation ($\Delta E_p = E_{pa} - E_{pc}$) of 66 mV and peak current ratios ($i_{pa}/i_{pc} = 1.8$) is consistent with quasi-reversibility with an electrochemical reduction followed by chemical reaction mechanism [55].

Acetaminophen displayed similar well-defined redox waves with dialysis covered and bare platinum electrodes. The peak potential and peak separation were identical which indicated that the electrode contacting dialysis membrane had no effect on electron transfer (Yin et al., 2010). However, peak currents were reduced

confirming a barrier effect. In parallel, cyclic voltammograms for the laminate covered electrodes showed a substantial decrease in peak current confirming the major reduction in diffusivity of the diffusant molecules (Fig. 3).

Complete electrolyte conductivity was not achieved until day 6, as indicated by a slow drifting baseline which restricted the time window for the sequence of CVs undertaken for any one membrane. The CVs for Loctite 3301 at day 15 (Fig. 4) are qualitatively similar to those observed with the other adhesives. Measurable peaks were demonstrated only at day 9 for hydrogen peroxide and oxygen, and at day 12 for the organics (Fig. 4 and Fig. 5).

3.3.3. Diffusion coefficients

In order to maintain consistency throughout the study, only the forward (anodic) peaks (cathodic for oxygen) were considered for diffusion coefficient calculations. Forward peaks are registered when the target molecule diffuses in through the adhesive from the bulk solution, whereas reverse peaks represent locally electrochemically generated product. The diffusion rate between these two could be starkly different owing to (i) a shift in molecular properties and/or (ii) insufficient electrochemical generation for distribution of product through the 'dead volume' presented by the covering film + dialysis void volume.

The pattern of change in permeability against time was similar for all adhesives, with no evident permeability initially, and a breakthrough effect on ageing with 9–12 days with an exponential increase in permeability, presumably coinciding with a critical pore generating phase. Importantly, the property separation across the organic vs non-organic groups was maintained, with possibly a marginally greater transport for oxygen as against the more polar hydrogen peroxide (Fig. 6). The consistency of these findings across

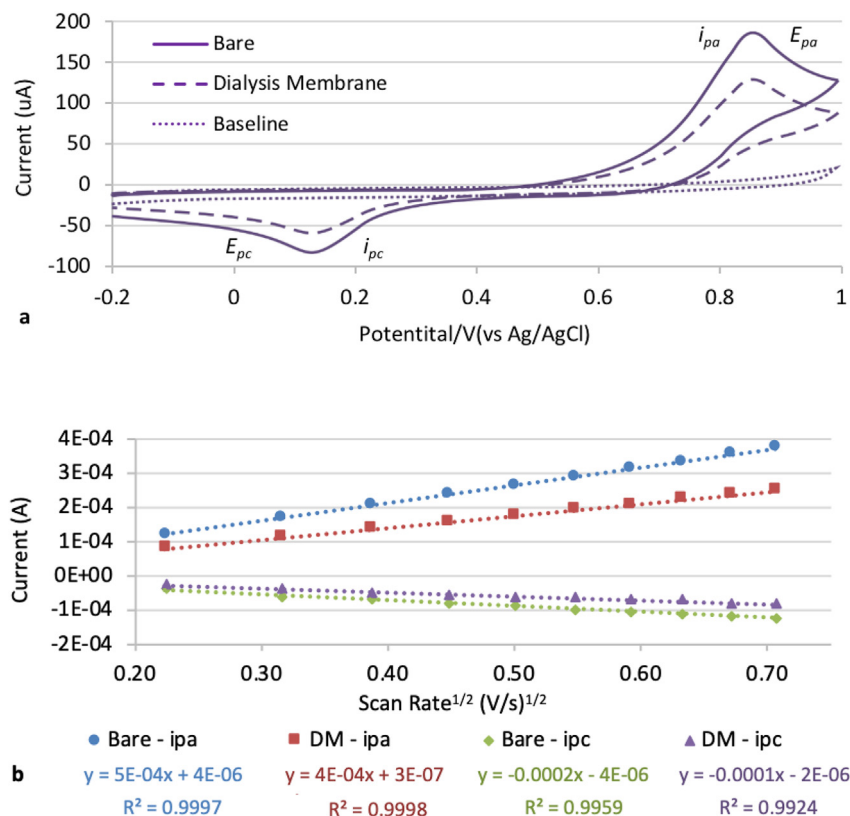


Fig. 3. CVs of acetaminophen (10 mM in PBS) at 100 mV/s vs Ag/AgCl showing (a) retained peak profile and (b) maintained diffusion control across a range of scan rates (100–500 mV/s) for a dialysis membrane covered Pt electrode.

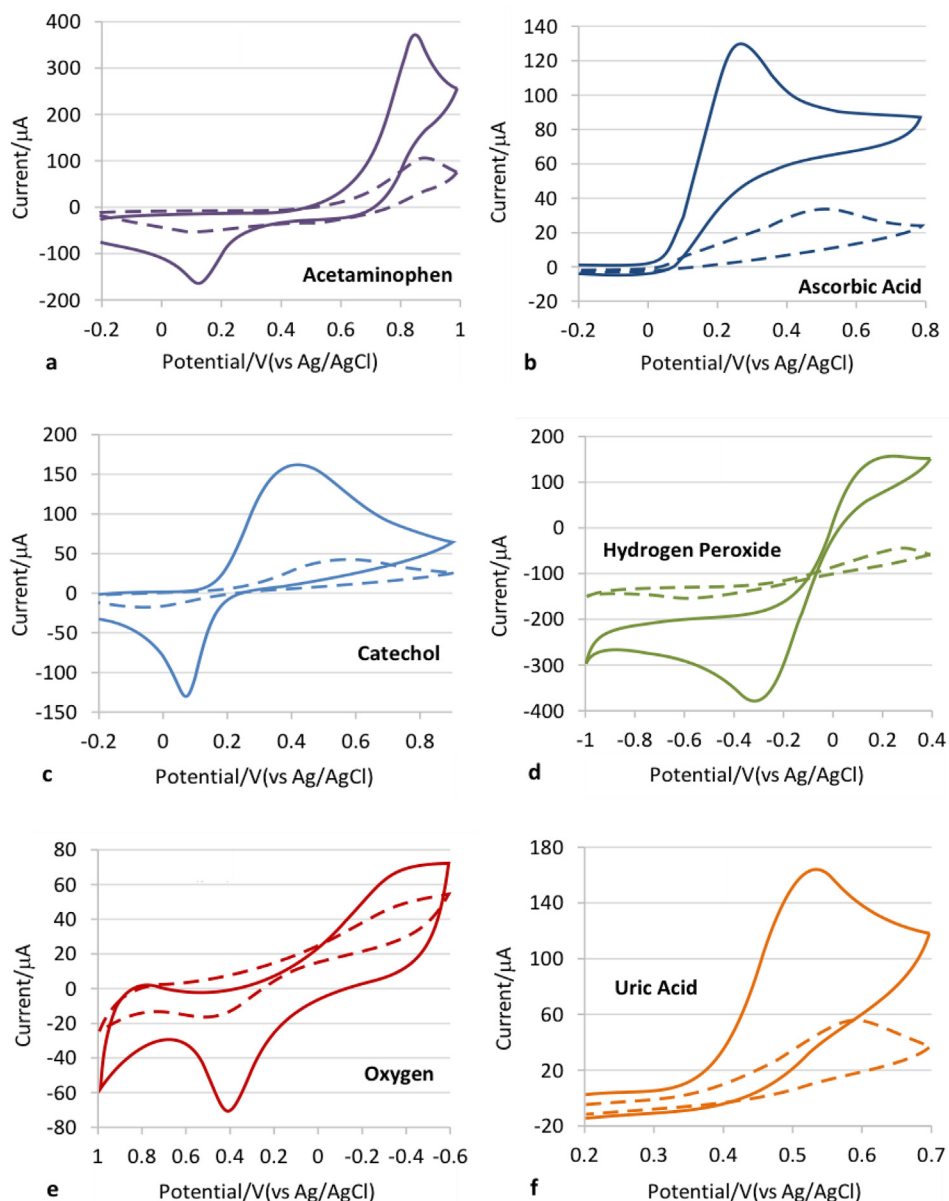


Fig. 4. Day 15 cyclic voltammograms (broken lines) of various analytes diffusing through Loctite 3301 adhesive membrane aged in Phosphate Buffer Solution (0.1 M, pH 7.4) at 37 °C. Solid lines, represent analytes diffusing through dialysis membrane. Scan rate: 100 mV/s.

the adhesive range shown in Fig. 7.

Whilst the trends are similar, a consistent difference in permeability is seen between the different adhesive types. However, notably, for the charged, diffusion through cyanoacrylate adhesive is faster than through acrylic and acrylate-urethane adhesives.

3.3.4. Strength measurement

Butt joints were susceptible to ageing effects at an earlier stage than lap shear joints (Fig. 7). These lost strength at day 6 compared to 9 days for the latter. In all cases, after the first loss in joint strength, subsequent losses were linear in contrast to the exponential permeability effects, and the greatest loss occurred with the more hydrophilic adhesives. Importantly, a clear (tenfold) increase in oxygen and hydrogen peroxide permeability (Fig. 7) is seen coinciding, at day 6, with the stage where strength starts to weaken, before the loss of strength accelerates significantly. So as a bulk property phenomenon, diffusion is more sensitive to

hydration change than adhesion as a surface integrity property.

4. Discussion

The uptake of water by a polymer is variously considered in terms of micro void uptake (*free volume theory*) and hydrogen bonding (*interaction theory*) [56–58]. The final steady state outcome is an equilibrium hydration state [59–61] defining general permeability behaviour. This is well recognised in the case of membrane based biosensors, where stable permeability and selectivity is attained within minutes on exposure to a sample and which, in the absence of fouling, offers relatively stable permeability and therefore response [62,63]. Water ingress prior to equilibration causes an accelerated permeability change which is known to have an exponential profile [64], and this was exactly observed for the hydrating adhesive polymers here. However, even for the dense adhesive layers used here, the hydration equilibrium

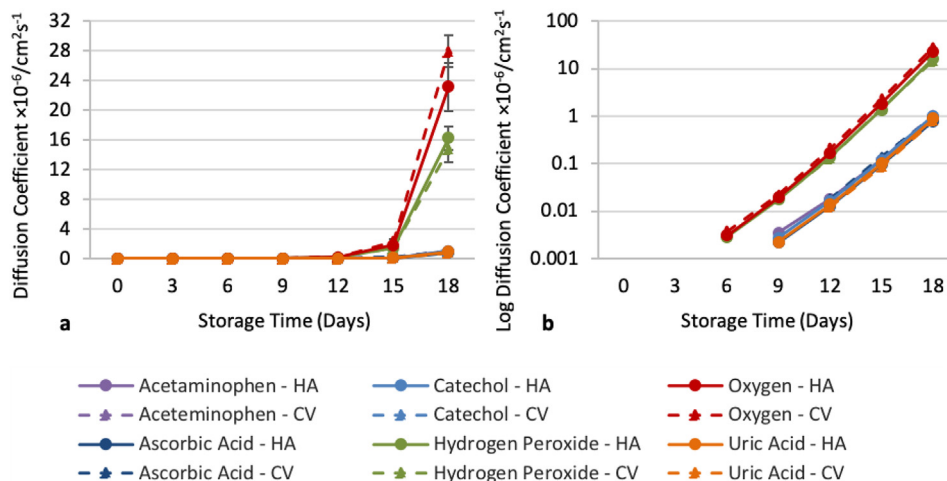


Fig. 5. Diffusion coefficients obtained via cyclic voltammetry (CV) and chronoamperometry.

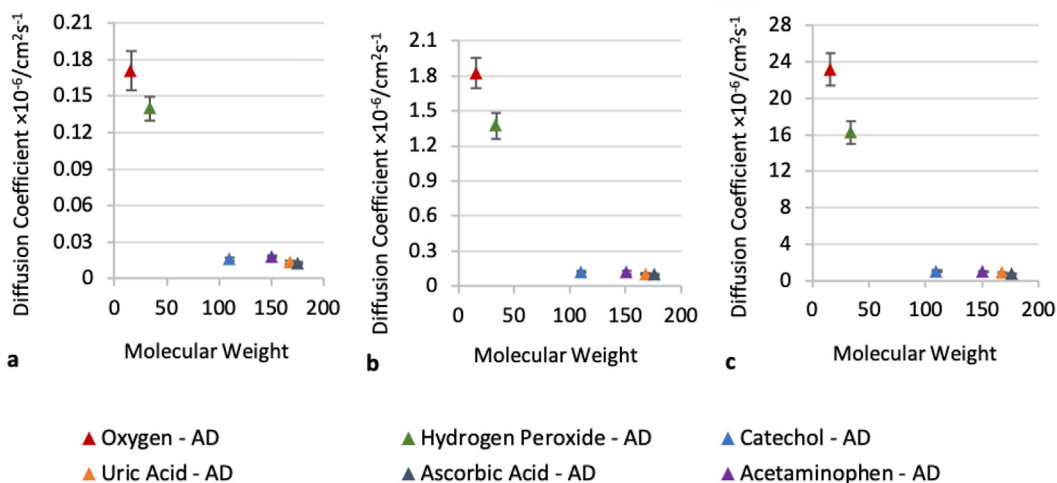


Fig. 6. Diffusion coefficients of analytes vs molecular weight through a Loctite 3301 adhesive membranes at various time periods during ageing for Loctite 3301 in PBS, 0.1 M, pH 7.4 at 37 °C; (a) day 12, (b) day 15 (c) day 18.

period for such thin layers would not be expected to continue for well beyond a week, and moreover would show dependence on hydrophilicity. This is evidently not the case with respect to the time of permeability initiation (Fig. 7). This supports the possibility of degradative changes in the pH 7.4 buffer, though any contribution of leachables loss cannot be discounted.

For such tightly controlled barriers with markedly reduced diffusion profiles for low molecular weight organics as compared with that in water, some discrimination would be expected against weight, charge, polarity and perhaps even aromatic group content (Fig. 6). Surprisingly, no such discrimination is seen, and further mechanistic analysis is warranted in the future together with high resolution structure analysis and BET. The fact that oxygen and hydrogen peroxide are profoundly different suggests a distinctly different transport mechanism. Thus, it is possible that transport, in addition to that through the adhesive voids, also occurs through the polymer matrix. This has implications for barrier membranes used for oxidase based first generation biosensors where greater oxygen permeability is demanded and observed, as compared with substrate to reduce co-substrate limitation. Quantitative analysis at low permeability systems such as these is demanding, but the agreement between the CV and amperometry studies indicates that

meaningful interpretation is possible.

Further analysis of larger molecular weight species is required in order to determine higher molecular weight access at further, extended, ageing periods. This has future importance for the period when there is partial bridging of the fracture surfaces, and adhesive joint is partly degraded; it is at this stage that biomolecule crosstalk for healing and remodelling of bone may become especially important. The fact, also, that oxygen permeability provided the earliest indication of porosity change is further in line with the high tendency of all polymer barriers to allow gas transport [65] even if other solutes are blocked, and may allow even a non-degraded adhesive to permit oxygen cellular access to a mostly vascular disrupted tissue field.

H_2O_2 :ascorbate diffusion coefficient ratio was 7:1 on day 12 and 15:1 on day 18. This indicates a higher sensitivity of small molecule monitoring for ageing and suggests that the non-pore mechanism for transport may be further augmented by ageing, assuming that the organics are only able to transfer through physical pores and not between polymer chains.

The generally accepted cut-off for surface wetting vs de-wetting by an adhesive is a 90° water contact angle [66]. All the contact angles here were below this value indicating a capacity for

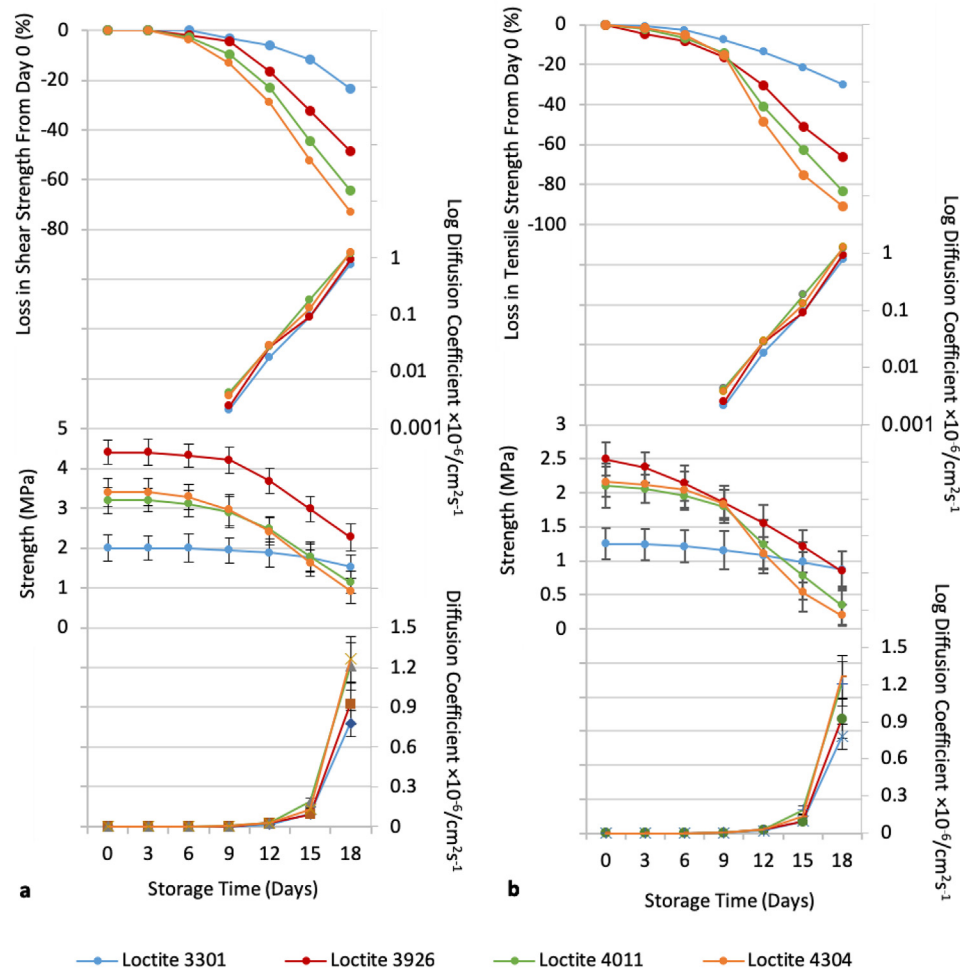


Fig. 7. a) Single Joint Lap Shear Strengths and b) Tensile Butt Strengths of cyanoacrylate adhesives to bone, along with diffusion coefficients (DC) of ascorbic acid across the full range of adhesives, aged in PBS, 0.1 M, pH 7.4 at 37 °C for up to 18 days (n = 7).

substrate penetration and wetting of a hydrophilic surface such as mineral bone. Differences in polarity, however, were not reflected in initial strength differences even though both are referable to interfacial properties (Fig. 7).

This study has determined *effective* diffusion coefficients (permeability) and does not compensate for solute partition variation. The polymeric adhesives are porous and may have been subject to partitioning increase as the polymers aged, but the measurements here provide the physically relevant measure of transport.

The strong correlation between permeability and adhesive joint strength was not expected, since the former is a bulk property whilst the latter is predominantly a surface phenomenon. The nature of the bone substrate adds another set of variables to confound the correlation; bone is a hydrophilic, porous structure able to absorb water and trap water which then serves as a variable surface hydration source [67,68], inevitably with maximal effect at the interface, and minimum effect in the bulk. Shear strength loss is more marked than that of tensile strength (Fig. 7). This may have been because of differences in water uptake from bone since surface contact was with aligned vs transected Haversian systems, though edge exposure to water was also geometrically different. Whilst permeability has a prime relevance for use in any biosensor, the added value of adhesion is the ability to create membrane laminates with mechanical integrity; certainly for extended use

and as flexible interfaces [69], however stable a barrier material, a failure to retain stable adhesion to contiguous layers is a potential drawback.

5. Conclusion

This is the first study to use permeability analysis as a bridge to mechanics; the finding of permeability initiation coinciding with joint weakening is an important indicator of hydration outcome, and has implications for all barrier materials, including those used in sensing. Molecular selectivity, as seen here for O_2 and H_2O_2 , could be a basis for evaluating porosity and warrants use of a wider library of probe molecules. Extension to large molecule studies will enable study of the stage at which cell signalling molecules are transported across an adhesive joint, and the strength properties this is associated with. Such studies could also serve as the basis for designing adhesives that are capable of creating more stable laminates for biosensing, beyond their more obvious application for fracture fixation.

Declaration of interests

The authors declare that they have no known competing financial interests or personal relationships that could have appeared to influence the work reported in this paper.

Acknowledgements

The authors wish to thank the EPSRC and TWI for generous support of a studentship for MR during this study, Henkel Ltd (Hemel Hempstead, UK for the donation of adhesives. Support in the development of electrochemical methods was provided by the EPSRC-NIHR "Medical Device and Vulnerable Skin" Network (Ref. EP/M000303/1).

Appendix A. Supplementary data

Supplementary data to this article can be found online at <https://doi.org/10.1016/j.acax.2019.100009>.

References

- [1] A.J. Teo, A. Mishra, I. Park, Y.-J. Kim, W.-T. Park, Y.-J. Yoon, Polymeric biomaterials for medical implants and devices, *ACS Biomater. Sci. Eng.* 2 (2016) 454–472.
- [2] I.C. Lopes, A. Zebda, P. Vadgama, New directions in membrane designs for biosensors, *Current Opinion in Electrochemistry* 2 (2018), <https://doi.org/10.1016/j.coelec.2018.07.009>.
- [3] Bone Health and Osteoporosis, A Report of the Surgeon General 12 (2004). Rockville MD.
- [4] C. Heiss, N. Hahn, S. Wenisch, V. Alt, P. Pokinskyj, U. Horas, O. Kilian, R. Schnettler, The tissue response to an alkylene bis(dilactoyl)-methacrylate bone adhesive, *Biomaterials* 26 (2005) 1389–1396.
- [5] B. Behm, P. Babilas, M. Landthaler, S. Schreml, Cytokines, chemokines and growth factors in wound healing, *J. Eur. Acad. Dermatol. Venereol.* 26 (2012) 812–820.
- [6] P. Niethammer, C. Grabher, A.T. Look, T.J. Mitchison, A tissue-scale gradient of hydrogen peroxide mediates rapid wound detection in zebrafish, *Nature* 459 (2009) 996.
- [7] A. Alghanem, G. Fernandes, M. Visser, R. Dziak, W.G. Renné, C. Sabatini, Biocompatibility and bond degradation of poly-acrylic acid coated copper iodide-adhesives, *Dent. Mater.* 33 (2017) e336–e347.
- [8] J.L. Cameron, S.C. Woodward, E.J. Pulaski, H.K. Sleeman, G. Brandes, R.K. Kulkarni, F. Leonard, The degradation of cyanoacrylate tissue adhesive, *Int. Surg.* 58 (1965) 424–430.
- [9] H.E. Koschwanez, W.M. Reichert, In vitro, in vivo and post explantation testing of glucose-detecting biosensors: current methods and recommendations, *Biomaterials* 28 (2007) 3687–3703.
- [10] U. Kandalam, A.J. Bouvier, S.B. Casas, R.L. Smith, A.M. Gallego, J.K. Rothrock, J.Y. Thompson, C.Y. Huang, E.J. Stelnicki, Novel bone adhesives: a comparison of bond strengths in vitro, *Int. J. Oral Maxillofac. Surg.* 42 (2013) 1054–1059.
- [11] S. Saska, E. Hochuli-Vieira, A. Minarelli-Gaspar, M.F.R. Gabrielli, M.V. Capela, M. Gabrielli, Fixation of autogenous bone grafts with ethyl-cyanoacrylate glue or titanium screws in the calvaria of rabbits, *Int. J. Oral Maxillofac. Surg.* 38 (2009) 180–186.
- [12] J.V. Quinn, *Tissue Adhesives in Clinical Medicine*, BC Decker, Incorporated, 2005.
- [13] J.C. Salamone, *Concise Polymeric Materials Encyclopedia*, Taylor & Francis, 1998.
- [14] S. Dumitriu, *Polymeric Biomaterials, Revised and Expanded*, CRC Press, 2001.
- [15] S.K. Bhatia, *Biomaterials for Clinical Applications*, Springer New York, 2010.
- [16] M. Donkerwolcke, F. Burny, D. Muster, Tissues and bone adhesives—historical aspects, *Biomaterials* 19 (1998) 1461–1466.
- [17] D.F. Farrar, Bone adhesives for trauma surgery: a review of challenges and developments, *Int. J. Adhesion Adhes.* 33 (2012) 89–97.
- [18] G.M. Brauer, J.W. Kumpula, D.J. Termini, K.M. Davidson, Durability of the bond between bone and various 2-cyanoacrylates in an aqueous environment, *J. Biomed. Mater. Res.* 13 (1979) 593–606.
- [19] J. Kilpikari, M. Lapinsuo, P. Tormala, H. Patiala, P. Rokkanen, Bonding strength of alkyl-2-cyanoacrylates to bone in vitro, *J. Biomed. Mater. Res.* 20 (1986) 1095–1102.
- [20] C. Evans, G. Lees, I. Trail, Cytotoxicity of cyanoacrylate adhesives to cultured tendon cells, *J. Hand Surg.* 24 (1999) 658–661.
- [21] L. Montanaro, C.R. Arciola, E. Cenni, G. Ciapetti, F. Savioli, F. Filippini, L.A. Barsanti, Cytotoxicity, blood compatibility and antimicrobial activity of two cyanoacrylate glues for surgical use, *Biomaterials* 22 (2000) 59–66.
- [22] C. O'Sullivan, C. Birkinshaw, Hydrolysis of poly (n-butylcyanoacrylate) nanoparticles using esterase, *Polym. Degrad. Stabil.* 78 (2002) 7–15.
- [23] S. Dumitriu, V.I. Popa, *Polymeric Biomaterials*, CRC Press/Taylor & Francis, 2013.
- [24] M.C. Harper, M. Ralston, Isobutyl 2-cyanoacrylate as an osseous adhesive in the repair of osteochondral fractures, *J. Biomed. Mater. Res. A* 17 (1983) 167–177.
- [25] M.A. Sermak, L. Wong, N. Inoue, B.J. Crain, M.J. Im, E.Y. Chao, P.N. Manson, Fixation of the craniofacial skeleton with butyl-2-cyanoacrylate and its effects on histotoxicity and healing, *Plast. Reconstr. Surg.* 102 (1998) 309–318.
- [26] S.R. Mobley, J. Hilinski, D.M. Toriumi, Surgical tissue adhesives, *Facial plastic surgery clinics of North America* 10 (2002) 147–154.
- [27] S.C.d. Souza, C.H. Briglia, Comparative study of the use of ethyl cyanoacrylate adhesive and intracutaneous suture for cutaneous excision closure, *Rev. Bras. Cienc. Poitica* 26 (2011) 566–572.
- [28] A. Nordberg, P. Antoni, M.I. Montanez, A. Hult, H. Von Holst, M. Malkoch, Highly adhesive phenolic compounds as interfacial primers for bone fracture fixations, *ACS Appl. Mater. Interfaces* 2 (2010) 654–657.
- [29] A. Pizzi, K.L. Mittal, *Handbook of Adhesive Technology, Revised and Expanded*, Taylor & Francis, 2003.
- [30] T.Ç. Çanak, E. Kıraylar, İ.E. Serhatlı, Preparation and application of urethane acrylate coatings for enhancing mechanical properties of coagulated surfaces, *Karaelmas Science & Engineering Journal* 6 (2016).
- [31] M. Unemori, Y. Matsuya, S. Matsuya, A. Akashi, A. Akamine, Water absorption of poly(methyl methacrylate) containing 4-methacryloxyethyl trimellitic anhydride, *Biomaterials* 24 (2003) 1381–1387.
- [32] A.J. Feilzer, A.I. Kakaboura, A.J. de Gee, C.L. Davidson, The influence of water sorption on the development of setting shrinkage stress in traditional and resin-modified glass ionomer cements, *Dent. Mater.* 11 (1995) 186–190.
- [33] A.J. Feilzer, A.J. De Gee, C.L. Davidson, Curing contraction of composites and glass-ionomer cements, *J. Prosthet. Dent* 59 (1988) 297–300.
- [34] S.A. Hanifah, L.Y. Heng, M. Ahmad, Biosensors for phenolic compounds by immobilization of tyrosinase in photocurable methacrylic-acrylic membranes of varying hydrophilicities, *Anal. Sci.* 25 (2009) 779–784.
- [35] F. Ismail, A. Willows, M. Khurana, P.E. Tomlins, S. James, S. Mikhailovsky, P. Vadgama, A test method to monitor in vitro storage and degradation effects on a skin substitute, *Med. Eng. Phys.* 30 (2008) 640–646.
- [36] Z. Rong, P. Vadgama, Bipartite expressions for diffusional mass transport in biomembranes, *Biophys. J.* 91 (2006) 4690–4696.
- [37] Z. Rong, P. Vadgama, An electrochemical method for measurement of mass transport in polymer membranes using acetaminophen as a model system, *Electrochim. Acta* 54 (2009) 4949–4953.
- [38] F. Ismail, A. Willows, M. Khurana, P. Tomlins, S. James, S. Mikhailovsky, P. Vadgama, A test method to monitor in vitro storage and degradation effects on a skin substitute, *Med. Eng. Phys.* 30 (2008) 640–646.
- [39] S. Sambandam, J. Parrondo, V. Ramani, Estimation of electrode ionomer oxygen permeability and ionomer-phase oxygen transport resistance in polymer electrolyte fuel cells, *Phys. Chem. Chem. Phys.* 15 (2013) 14994–15002.
- [40] A.J. Bard, L.R. Faulkner, *Electrochemical Methods: Fundamentals and Applications*, Wiley, 2000.
- [41] X. Yuan, N. Xu, Determination of hydrogen diffusion coefficient in metal hydride electrode by cyclic voltammetry, *J. Alloy. Comp.* 316 (2001) 113–117.
- [42] X.H. Rui, N. Ding, J. Liu, C. Li, C.H. Chen, Analysis of the chemical diffusion coefficient of lithium ions in LiV2(PO4)3 cathode material, *Electrochim. Acta* 55 (2010) 2384–2390.
- [43] N. Ding, J. Xu, Y.X. Yao, G. Wegner, X. Fang, C.H. Chen, I. Lieberwirth, Determination of the diffusion coefficient of lithium ions in nano-Si, *Solid State Ionics* 180 (2009) 222–225.
- [44] Z. Rong, S. Rashid, P. Vadgama, A bipartite expression for the transient amperometric current at a membrane covered planar electrode to characterize solute diffusion through the membrane, *Electroanalysis* 18 (2006) 1703–1709.
- [45] Z. Rong, P. Vadgama, Bipartite expressions for amperometric currents of recessed, membrane covered planar and hanging mercury drop electrodes, *J. Electroanal. Chem.* 614 (2008) 166–170.
- [46] A.T. Haug, R.E. White, Oxygen diffusion coefficient and solubility in a new proton exchange membrane, *J. Electrochem. Soc.* 147 (2000) 980–983.
- [47] M.C. Kimble, R.E. White, Y.M. Tsou, R.N. Beaver, Estimation of the diffusion coefficient and solubility for a gas diffusing through a membrane, *J. Electrochem. Soc.* 137 (1990) 2510–2514.
- [48] V. Compañ, M.A. Villar, E. Vallés, E. Riande, Permeability and diffusional studies on silicone polymer networks with controlled dangling chains, *Polymer* 37 (1996) 101–107.
- [49] J. Guzmán, M.T. Iglesias, E. Riande, V. Compañ, A. Andrio, Synthesis and polymerization of acrylic monomers with hydrophilic long side groups. Oxygen transport through water swollen membranes prepared from these polymers, *Polymer* 38 (1997) 5227–5232.
- [50] A. Yaroshchuk, Y. Boiko, A. Makovetskiy, Electrochemical perm-selectivity of active layers and diffusion permeability of supports of an asymmetric and a composite NF membrane studied by concentration-step method, *Desalination* 245 (2009) 374–387.
- [51] C. Schoo, M. Knoll, New simple electrochemical method for measuring the water vapor transmission rate and diffusion coefficient of polymer membranes, *Sensor Actuator Phys.* 225 (2015) 20–24.
- [52] J. Peron, A. Mani, X. Zhao, D. Edwards, M. Adachi, T. Soboleva, Z. Shi, Z. Xie, T. Navessin, S. Holdcroft, Properties of Nafion® NR-211 membranes for PEMFCs, *J. Membr. Sci.* 356 (2010) 44–51.
- [53] M.R. Carrilho, F.R. Tay, A.M. Donnelly, K.A. Agee, R.M. Carvalho, K. Hosaka, A. Reis, A.D. Loguercio, D.H. Pashley, Membrane permeability properties of dental adhesive films, *Journal of Biomedical materials Research Part B: applied biomaterials: an Official Journal of the Society for biomaterials, The Japanese Society for Biomaterials, and The Australian Society for Biomaterials and the Korean Society for Biomaterials* 88 (2009) 312–320.
- [54] C. Gary-Bobo, R. DiPollo, A. Solomon, Role of hydrogen-bonding in nonelectrolyte diffusion through dense artificial membranes, *J. Gen. Physiol.* 54 (1969)

- 369–382.
- [55] H. Filik, A.A. Avan, S. Aydar, G. Çetintaş, Determination of acetaminophen in the presence of ascorbic acid using a glassy carbon electrode modified with poly (caffeic acid), *Int. J. Electrochem. Sci* 9 (2014) 148–160.
- [56] S. Venz, B. Dickens, NIR-spectroscopic investigation of water sorption characteristics of dental resins and composites, *J. Biomed. Mater. Res.* 25 (1991) 1231–1248.
- [57] N. Marcovich, M. Reboledo, M. Aranguren, Moisture diffusion in polyester–woodflour composites, *Polymer* 40 (1999) 7313–7320.
- [58] R.E. Kerby, L.A. Knobloch, S. Schrickler, B. Gregg, Synthesis and evaluation of modified urethane dimethacrylate resins with reduced water sorption and solubility, *Dent. Mater.* 25 (2009) 302–313.
- [59] S. Deb, M. Braden, W. Bonfield, Water absorption characteristics of modified hydroxyapatite bone cements, *Biomaterials* 16 (1995) 1095–1100.
- [60] R.E. Shalin, *Polymer Matrix Composites*, Springer, 1995.
- [61] I.D. Sideridou, M.M. Karabela, D.N. Bikiaris, Aging studies of light cured dimethacrylate-based dental resins and a resin composite in water or ethanol/water, *Dent. Mater.* 23 (2007) 1142–1149.
- [62] S. Anastasova, A.-M. Spehar-Déleze, D. Bickham, P. Uebel, M. Schmidt, P. Russell, P. Vadgama, Stabilised biosensing using needle-based recess electrodes, *Electroanalysis* 24 (2012) 529–538.
- [63] B. Yu, Y. Moussy, F. Moussy, Lifetime improvement of glucose biosensor by epoxy-enhanced PVC membrane, *Electroanalysis: An International Journal Devoted to Fundamental and Practical Aspects of Electroanalysis* 17 (2005) 1771–1779.
- [64] J. Siepmann, R.A. Siegel, M.J. Rathbone, *Fundamentals and Applications of Controlled Release Drug Delivery*, Springer, 2011.
- [65] D.H. Kim, Y.S. Ryu, S.H. Kim, Improvements in the Oxygen Barrier Property of Polypropylene Nanocomposites, *Polymers for Advanced Technologies*, 2018.
- [66] Y. Yuan, T.R. Lee, Contact Angle and Wetting Properties 51 (2013) 3–34.
- [67] M. Bowditch, The durability of adhesive joints in the presence of water, *Int. J. Adhesion Adhes.* 16 (1996) 73–79.
- [68] E.M. Knox, M.J. Cowling, Durability aspects of adhesively bonded thick adherend lap shear joints, *Int. J. Adhesion Adhes.* 20 (2000) 323–331.
- [69] E.L. Tur-García, F. Davis, S.D. Collyer, J.L. Holmes, H. Barr, S.P. Higson, Novel flexible enzyme laminate-based sensor for analysis of lactate in sweat, *Sensor. Actuator. B Chem.* 242 (2017) 502–510.